International Journal of Thermophysics, Vol. 13, No. 3, 1992

Measurement of the Thermal Diffusivity of Thin Films on Substrate by the Photoacoustic Method

M. Akabori,[1] Y. Nagasaka,[1] and A. Nagashima[1]

Received October 3, 1991

Measurements of the thermal diffusivity of thin films on substrate have been performed by the photoacoustic method. In order to examine the method we have built a new apparatus and proposed (1) a system calibration procedure using optically and thermally thick reference samples and (2) a data analysis procedure based on the RG (Rosencwaig and Gersho) theory. As a result of using a transparent photoacoustic cell, the systematic errors which are caused by stray light have been reduced. With this apparatus, measurements have been performed on platinum, titanium, and stainless steel (SUS304) thin foils (thickness form 50 to 100 μm) with three different liquid backing materials (water, glycerol, and ethyl alcohol). The reproducibility was within $\pm 7\%$ regardless of film thickness and substrate materials.

KEY WORDS: photoacoustic method; RG (Rosencwaig and Gersho) theory; thermal diffusivity; thin film on substrate.

1. INTRODUCTION

In the recent advanced technologies, thermophysical properties of thin films of semiconductors, metals, and oxides are needed for several research fields, such as the thermal design of high chip-gate density ULSI [1] and array-type laser diodes [2] and the heat flow analysis of pulsed-laser-induced damage of optical thin films [3–6]. In order to analyze heat transfer problems in microscale electronic devices and to estimate damage thresholds of optical thin coatings, it is essential to know accurately the thermophysical properties (especially thermal conductivity and thermal diffusivity) of thin films under *in situ* conditions.

[1] Department of Mechanical Engineering, Keio University, 3-14-1 Hiyoshi, Yokohama 223, Japan.

0195-928X/92/0500-0499$06.50/0

However, the thermal properties (transport properties) of thin solid films can be several orders of magnitude lower than that of corresponding material in bulk form as a consequence of the film microstructures (grain boundaries, voids, and microcracks), which stems primarily from the deposition process such as chemical vapor deposition (CVD) or sputtering [3–6]. Some microstructure models have been presented to interpret this considerable decrease in the thermal conductivity and thermal diffusivity of thin films [7, 8]. Therefore, it is necessary to measure the thermal conductivity for each film *in situ* and not to use a "literature value for bulk" for a given material.

The conventional measurement techniques cannot be aplied to the thin films on substrate because they are too thin to attach heaters and temperature sensors on them. Up to now, the thermal conductivity and thermal diffusivity of thin films have been measured with the aid of the steady-state method [7], thermal comparator method [3, 6], AC calorimetric method [10], laser flash method [11], and radiation heat exchange method [12]. These methods are applicable primarily to free-standing thin films, and in some cases the temperature sensor such as a thin thermocouple should be attached to the sample surface.

In order to solve the above-mentioned problems, we have developed the photoacoustic method to measure the thermal diffusivity of solid thin films on substrate without special sample treatment. The advantages of the applications of the photoacoustic method to the measurements of the thermophysical properties of thin films are summarized as follows. (i) It is not necessary to attach temperature sensors to the sample (contact-free). (ii) The method can be applicable to thin films on substrate with no special sample treatment (*in situ* and nondestructive). (iii) Thermal diffusivity (perpendicular to the surface) of thin films can be determined without prior information on substrate. In addition, if we know the thermal conductivity and thermal diffusivity of the substrate, we can simultaneously determine the thermal conductivity of thin films. In spite of these advantages, the photoacoustic method has not been applied to the measurement of thermal properties of thin films on substrate except for a few studies [13, 14]. The main applications of this method have been limited to spectroscopy and other fields without regard to the thermal properties [15–17].

The photoacoustic measurement of the thermal diffusivity is that the thermal wave (AC component of the temperature of periodically heated sample) is generated inside the sample as a result of the absorption of an amplitude-modulated light beam. The heat conduction process is investigated through the variation in amplitude and phase lag of the surface temperature of the sample. This variation is detected as a pressure change (sound) inside the cell which is caused by a temperature variation

in a thin layer of the gas at the gas–sample boundary. This method is capable of detecting AC temperature amplitudes of 10^{-6} to 10^{-5} K.

The purpose of the present study is to establish the photoacoustic method as a technique to measure the thermal diffusivity of thin films (μm order thickness) on substrate. As an initial step, we have developed a new photoacoustic instrument and a data analysis procedure for measuring thermal diffusivity of thin films on substrate.

2. PRINCIPLE OF MEASUREMENT

Figure 1 schematically shows an idealized configuration of a photoacoustic cell. A thin film or sample (thickness l_s) is mounted so that its front surface is exposed to a gas (normally air, thickness l_g) and is attached on a backing material (substrate) of thickness l_b. When the sample contained in a gas-tight cell is periodically heated by a modulated light source, periodic heat flow from the sample causes a temperature variation in a thin layer of the gas at the gas–sample boundary. The resulting piston-like behavior of this layer induces a periodic overpressure of gas in the cell, which is detected as a sound. This phenomenon is called photoacoustic (PA) effect and the photoacoustic signals (amplitude and phase) contain information about (i) the thermophysical properties, (ii) optical properties (absorption coefficient), and (iii) the thickness of the thin film, substrate and gas. Therefore, if we measure the PA signals as a function of modulation frequency of the incident light and use appropriate data analysis, it is in principle possible to extract the thermophysical properties of the thin film.

The first theoretical treatment of the photoacoustic effect was established by Rosencwaig and Gersho in 1976 [18] (referred to as the RG

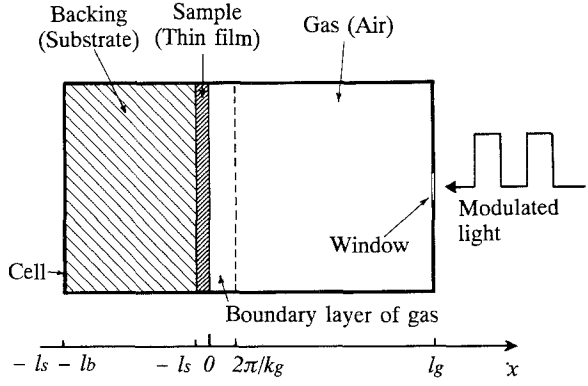

Fig. 1. One-dimensional model of a photoacoustic cell.

theory). Since the present study is based on the RG theory, we briefly summarize the theory. The RG theory assumes the following idealized conditions: (i) heat conduction is one-dimensional within the gas, sample, and backing layers with respect to the AC component, (ii) the gas and backing materials are not light absorbing, (iii) absorbed light energy is instantaneously converted into heat in the sample, (iv) the length of the gas column is much greater than the thermal diffusion length in the gas ($\mu_g \ll l_g$), (v) the effect of thermal expansion of the sample is negligible, (vi) no thermal contact resistance exists between the sample and the backing, (vii) no convection in the gas surrounding the sample, and (viii) no radiation heat loss from the sample. It should be mentioned that these assumptions are practically satisfied in the actual PA cell configurations except for high-temperature conditions.

When the sample is irradiated by the monochromic light of wavelength λ_h with intensity I_0 [$\mathrm{W \cdot m^{-2}}$] sinusoidally modulated at frequency ω, we can express the variation of light intensity I as

$$I = \tfrac{1}{2} I_0 (1 + \cos \omega t) \tag{1}$$

The heat generated at point x, $\dot{q}$ [$\mathrm{W \cdot m^{-3}}$], due to light absorption in the sample is given by

$$\dot{q} = \tfrac{1}{2} \beta I_0 \exp \beta x (1 + \cos \omega t) \tag{2}$$

where β denotes the absorption coefficient of the sample for λ_h. If we assume one-dimensional heat conduction within three layers and that all the absorbed light is instantaneously converted into thermal energy, the basic problems are governed by the following Fourier equations with respect to the complex temperature Φ.

$$\frac{\partial^2 \Phi_s}{\partial x^2} = \frac{1}{a_s} \frac{\partial \Phi_s}{\partial t} - \frac{\beta I_0}{2\lambda_s} \exp \beta x (1 + \exp j\omega t), \qquad -l_s \leqslant x \leqslant 0 \tag{3}$$

$$\frac{\partial^2 \Phi_b}{\partial x^2} = \frac{1}{a_b} \frac{\partial \Phi_b}{\partial t}, \qquad -(l_s + l_b) \leqslant x \leqslant -l_s \tag{4}$$

$$\frac{\partial^2 \Phi_g}{\partial x^2} = \frac{1}{a_g} \frac{\partial \Phi_g}{\partial t} \qquad 0 \leqslant x \leqslant l_g \tag{5}$$

where a is the thermal diffusivity, λ the thermal conductivity, and j the imaginary unit. The subscripts, s, g, and b denote the sample, gas, and backing material, respectively. The continuity conditions of temperature and heat flux at the two boundaries are

$$\Phi_s(0, t) = \Phi_g(0, t) \tag{6}$$

$$\Phi_s(-l_s, t) = \Phi_b(-l_s, t) \tag{7}$$

$$\lambda_s \frac{\partial \Phi_s}{\partial x}(0, t) = \lambda_g \frac{\partial \Phi_g}{\partial x}(0, t) \tag{8}$$

$$\lambda_s \frac{\partial \Phi_s}{\partial x}(-l_s, t) = \lambda_b \frac{\partial \Phi_b}{\partial x}(-l_s, t) \tag{9}$$

$$\Phi_b(-l_s - l_b, t) = 0 \tag{10}$$

$$\Phi_g(l_g, t) = 0 \tag{11}$$

Since the photoacoustic signal is produced by a modulated component (AC) of the temperature variation in the gas near the sample, the complex solution is given by

$$\Phi_{AC}(x, t) = \theta \exp(-\sigma_g x + j\omega t) \tag{12}$$

where

$$\theta = \frac{\beta I_0}{2\lambda_s(\beta^2 - \sigma_s^2)} \times \frac{(r-1)(b+1)\exp(\sigma_s l_s) - (r+1)(b-1)\exp(-\sigma_s l_s) + 2(b-r)\exp(-\beta l_s)}{(g+1)(b+1)\exp(\sigma_s l_s) - (g-1)(b-1)\exp(-\sigma_s l_s)} \tag{13}$$

Here we define the following parameters: $\sigma_i = (1+j)k_i$, the complex wave number of temperature wave in the material i; $k_i = \sqrt{\omega/2a_i}$, the wave number of material i (m^{-1}); $r = \beta/\sigma_s$; $b = e_b/e_s$, the ratio of the thermal effusivity of the backing to that of the sample; $g = e_g/e_s$; $e_i = (\lambda_i \cdot \varrho_i \cdot C_i)^{1/2}$, the thermal effusivity of material i ($W \cdot s^{1/2} \cdot m^{-2} \cdot K^{-1}$); C_i, the specific heat capacity at constant pressure of material i ($J \cdot kg^{-1} \cdot K^{-1}$); and ϱ_i, the density of material i ($kg \cdot m^{-3}$). The subscript i denotes s, g, and b, respectively.

The actual temperature distribution in the cell is given is given by the real part of the complex solution [19]. If we denote the real and imaginary parts of θ as θ_1 and θ_2, respectively, the AC component of temperature variation in the gas is given by

$$T_{AC}(x, t) = \exp(-k_g x)[\theta_1 \cos(\omega t - k_g x) - \theta_2 \sin(\omega t - k_g x)] \tag{14}$$

It can assumed that the thin boundary layer of the gas expands and contracts periodically and can be considered as acting like an acoustic piston

on the rest of the gas column, since the AC temperature variation T_{AC} fully decays within the distance of one wavelength $x = 2\pi/k_g$. Therefore, the final pressure variation (sound) is expressed as

$$\Delta P(t) = q \cos(\omega t - \pi/4 - \Delta\phi) \tag{15}$$

where q and $\Delta\phi$ denote the amplitude and the phase lag between modulated light and the sound, respectively, which are the absolute value and argument of Eq. (18).

$$\Delta\phi = \arg Q \tag{16}$$

$$q = |Q| \tag{17}$$

$$Q = \frac{\gamma P_0}{\sqrt{2} l_g k_g T_0} \theta \tag{18}$$

where γ is the ratio of specific heats of the gas, and P_0 and T_0 are the average pressure and the average temperature of the gas, respectively. This exact RG theory expresses the magnitude and phase lag of the photoacoustic signal as a function of the optical, thermal, and geometrical properties of the sample, backing, and gas within the cell. Consequently, by using Eqs. (13), (15), and (18) and applying the suitable data analysis procedure on the measured amplitude and phase lag as a function of modulation frequency, we can determine the thermophysical properties of the sample without knowing the thermophysical properties of the backing material and the gas.

In addition, this rather complicated phenomenon is well understood in terms of the interference of thermal waves generated in the sample [20], which means the superposition of simple harmonic solutions of the heat conduction equation.

3. DATA EXTRACTION PROCEDURE FROM THE PA PHASE LAG SIGNAL

3.1. Data Analysis Using the RG Theory Without Simplification

In order to visualize the rather complicated RG theory, Fig. 2 displays (a) the amplitude and (b) the phase lag of the photoacoustic signal as a function of nondimensional parameters $k_s l_s$ (implies thermal thickness of the sample), βl_s (implies the optical thickness of the sample), and b in the case of $\beta l_s = 100$. As can be seen from Fig. 2, the phase lag is much more sensitive to the variation of the thermophysical properties of the sample

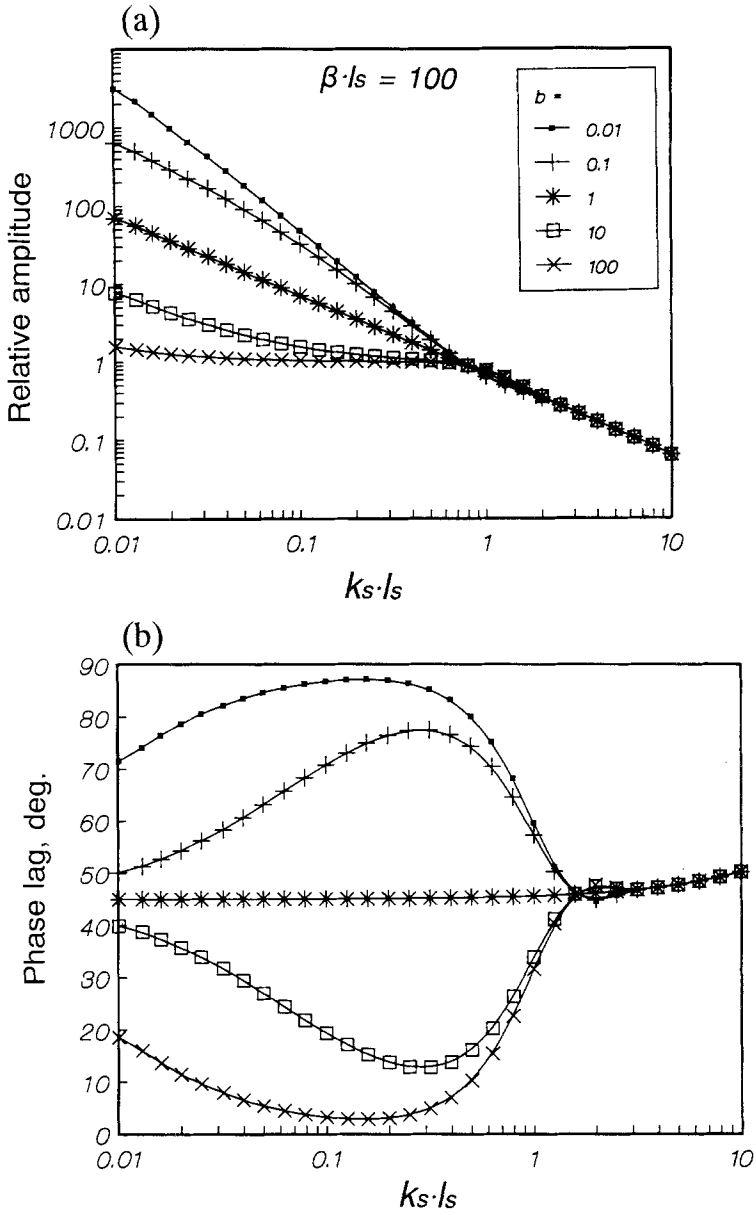

Fig. 2. (a) Amplitude and (b) phase lag of photoacoustic signal calculated by the RG theory using nondimensional parameters in the case of $\beta l_s = 100$.

than the amplitude. In the present study, therefore, we have chosen to analyze the phase lag in the photoacoustic signal to extract the thermal diffusivity of the sample.

By simplifying and summarizing the RG theory, the phase lag $\Delta\phi$ can be rewritten using the following four nondimensional parameters as

$$\Delta\phi = F(f: \beta l_s, k_s l_s/\sqrt{f}, b, g) \tag{19}$$

We can assume that $g = 0$ because the thermal effusivity of gas is neglected in comparison with that of the sample (i.e., $e_g \ll e_s$). The absorption coefficient of metallic sample β is of the order of 10^8 (m^{-1}), thus the absorption length $1/\beta$ is significantly smaller than the sample thickness of 50 to 100 μm. According to the RG theory, when $\beta l_s > 1000$ the sample is supposed to be optically thick, which means surface heating; the phase lag has almost no dependence on the parameter βl_s. Eventually, in the present study, the photoacoustic phase lag signal depends only on two parameters, namely, $k_s l_s/\sqrt{f}$ and b. If we suppose that the thickness of the sample l_s is known, unknown parameters are a_s and b. Therefore, as displayed in Fig. 3 (phase lag vs frequency for Ti sample of thickness 50 μm on water backing fitted to RG theory as a typical example), it is possible to determine a_s and b through the nonlinear least-squares curve fitting of measured phase lag data on the RG theory. Since the thermophysical properties of the backing material are implicitly included in the parameter b, it is possible to deter-

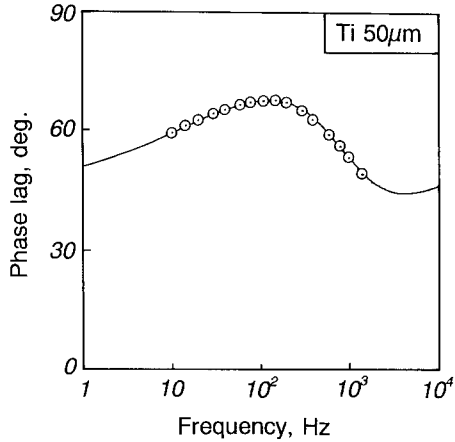

Fig. 3. An example of phase lag-vs-frequency data for titanium sample of thickness 50 μm on water backing. (⊙) Experimental data; (——) curve-fitting by the RG theory.

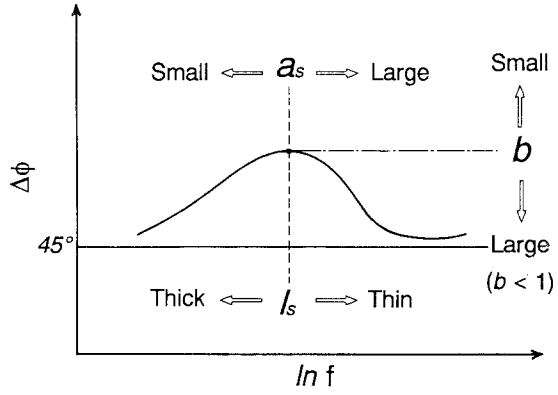

Fig. 4. Qualitative dependence of $\Delta\phi - \ln f$ curve on a_s, l_s, and b.

mine a_s without knowing the backing properties in advance. Moreover, we can simultaneously obtain the thermal conductivity of the sample, if we know the thermal effusivity of the backing e_b. Figure 4 qualitatively illustrates the dependence of the $\Delta\phi - \ln f$ curve on a_s, l_s, and b. Roughly speakinig, in the case of $b < 1$ the maximum point of the curve determines a_s or l_s and the height of the maximum point depends on b.

3.2. Cell Constant Calibration Using a Reference Sample

In the present apparatus, the photoacoustic signal is detected by a microphone and the phase lag is measured by a lock-in amplifier. In general, the measured phase lag data using such a system contain factors other than the phase lag described by the RG theory such as microphone response, effective thickness of the gas in the cell, instrumental phase offset, etc. It may be extremely difficult to measure directly the "absolute phase lag." Consequently, these apparatus-dependent effects need to be removed from the measured data by choosing an appropriate reference sample for a specific system configuration as a function of modulated frequency.

According to the RG theory, if a sample is optically thick ($l_s \gg 1/\beta$), thermally thick ($l_s \gg 1/k_s$), and $\beta \gg k_s$ (these conditions are usually satisfied for opaque bulk materials), the phase indicates $\pi/4$ regardless of modulation frequencies. Therefore by choosing the above-mentioned material as a reference sample, all the measured phase variations are attributed to the measurement system. Figure 5 demonstrates that the measured phase lag values for the reference samples such as bulk stainless steel (SUS304) and titanium agree quite well. This frequency-dependent phase lag is attributed to the present specific system.

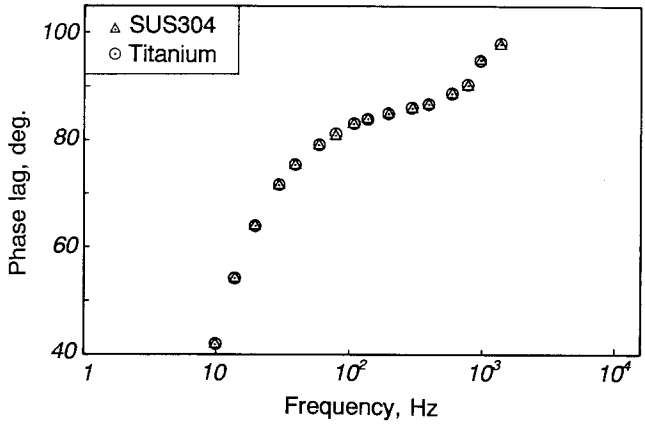

Fig. 5. Cell constant calibration using optically and thermally thick reference samples.

In the actual experimental procedure, the measurements are performed in two stages: system calibration and unknown sample measurement. First, the system calibration is accomplished using a reference sample and the frequency-dependent system characteristic factor $\Delta\phi_{\text{ref}}$ is determined so that the measured phase lag data amount to $\pi/4$. Second, the measurement for an unknown sample is performed as a function of frequency and the calibration phase data $\Delta\phi_{\text{ref}}$ are subtracted from the sample phase lag data $\Delta\phi_{\text{meas}}$. In this way we can cancel frequency-dependent phase shifts and systematic phase variations present in both measurements given in the following equation; thus the resultant phase difference $\Delta\phi$ characterizes the sample and substrate system alone, which is identical to the value calculated by the RG theory.

$$\Delta\phi = \Delta\phi_{\text{meas}} - \Delta\phi_{\text{ref}} + \pi/4 \tag{20}$$

It should be noted here that this calibration procedure may be used provided that the two measurements system are identical in terms of cell configurations, namely, cell volume, shape, and distance between beam spot and microphone.

4. MEASUREMENT SYSTEM

The functional diagram of the measurement system is shown in Fig. 6. The heating light source is a 1.2-W Ar^+ laser (514.5 nm), modulated by an acoust-optic modulator (AOM) operating from 10 to 1400 Hz in the present study. It is important to employ nonmechanical modulator in order

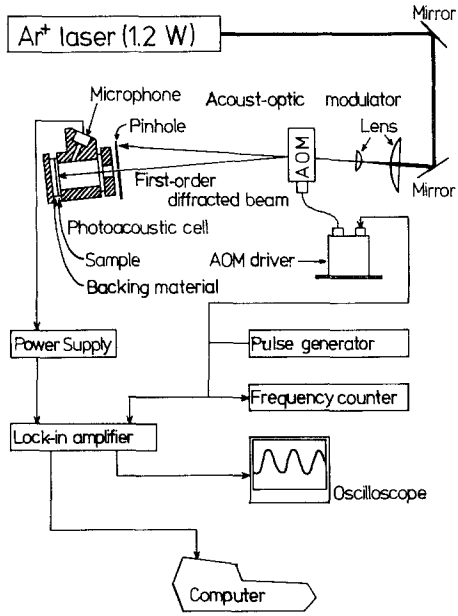

Fig. 6. Functional diagram of the measurement system.

to reduce the sound noise, especially under high chopping frequencies. The sample is placed in the photoacoustic cell (internal cell size is 12 mm in diameter and 12 mm in length) made of a transparent acrylic resin whose cross-section view is illustrated in Fig. 7.

The thin metallic foil sample (8) (50 to 100 μm in thickness) is attached on a sample holder and its backing materials are liquids (water,

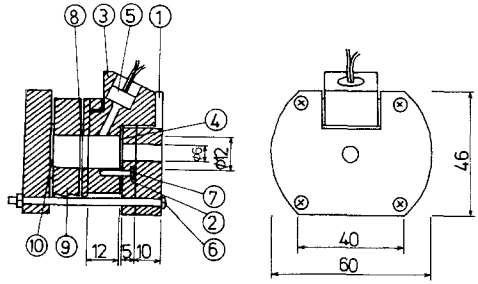

Fig. 7. Transparent photoacoustic cell. (1) Plate; (2) front cover; (3) cell body (acrylic resin); (4) Pyrex glass window; (5) condenser microphone; (6) sample holder screw; (7) window screw; (8) sample; (9) liquid backing chamber; (10) silicone rubber packing.

glycerin, and ethanol) in order to eliminate the thermal contact resistance between them. The photoacoustic sound is detected by a 10-mm condenser microphone (5). The signal is sent to a two-phase lock-in amplifier (PAR 5210) controlled by a personal computer. The entire apparatus is arranged on an optical bench.

5. EFFECTS OF STRAY-LIGHT

In the case of reflecting samples such as metals, their reflectivity is 50 to 90% at the wavelength of Ar^+ laser. Therefore, unexpected photoacoustic signal contributions from the cell walls generated by the light diffusively reflected (or stray light) at the sample surface cannot be neglected [21, 22]. These stray-light contributions cause the systematic shift and irregularity (fluctuation) of the measured phase lag. Moreover, these effects cannot be eliminated by the calibration procedure, because in two measurements the local distribution of the scattered light in the cell may be different and the photoacoustic signal contributions from cell walls also may differ for each measurement condition.

In order to determine the amount of the stray-light effects experimentally, we have measured the relative photoacoustic intensity of the stray-light component to the total photoacoustic sound in two types of cells, namely, an opaque cell made of brass and a transparent cell made of acrylic resin. Table I lists the results for three samples (SUS304, titanium, and aluminum). The method is that proposed by Krueger et al. [21] as follows. First, the total photoacoustic signals from the sample and the stray light are measured using the normal experimental setup. Then the photoacoustic signals from the sample are suppressed by placing a transparent glass layer on the sample, and therefore the only straight-light component signals are measured. As shown in Table I, using the transparent cell, we can reduce the effects of stray light to 1/10 in comparison with the opaque cell.

Table I. Comparison of the Stray-Light Components in the PA Signal Using a Brass Cell with Those Using an Acrylic Resin Cell

Sample	Brass cell (%)	Acrylic resin cell (%)
SUS304	19	1.9
Titanium	24	2.5
Aluminum	90	9.0

For this stray-light component, it seems impractical or impossible to apply theoretical correction or experimental cancellation. So in the present study we made a photoacoustic cell so that the stray-light signal becomes as small as possible. To reduce signal contributions due to light absorbed at the cell walls, the microphone, and other parts of the cell, we have employed the following scheme: (i) the cell body was made of a transparent acrylic resin and the O-ring material was semitransparent silicone rubber; (ii) The inner surface of the cell wall was adequately polished; and (iii) the microphone was separated from the gas volume by a narrow channel to protect it from the stray light. The resultant measured phase lag reproducibility has improved to be $\pm 0.1°$.

6. MEASUREMENTS OF METAL FOILS ON LIQUID BACKINGS

In order to confirm that the present photoacoustic instrument can be applied to the measurement of the thermal diffusivity of thin samples on substrate in accordance with the theory, we have employed three bulk metal foil samples together with three different liquid backing materials. The samples used were (i) stainless steel (SUS304) (thickness, 50 and 70 μm); (ii) titanium, which has a stated purity of 99.5% (thickness, 50 and 100 μm); and (iii) platinum, which has a stated purity of 99.98% (thickness, 100 μm). Additionally, all these samples were made by the rolling process, which means that the samples may have retained their "bulk properties." In order to avoid the thermal contact resistance between the sample and the backing, we have chosen liquids (water, glycerol, and ethanol) as backing materials since the aim of the present study is to check

Table II. Experimental Results on Thermal Diffisivity and b (in Parentheses) of Metal Foils on Three Liquid Backing Materials

Sample	Thickness (μm)	Thermal diffusivity ($b = e_b/e_s$) ($m^2 \cdot s^{-1}$)		
		Water	Glycerin	Ethanol
SUS304	50	2.60×10^{-6} (0.269)	2.56×10^{-6} (0.167)	—
	70	2.65×10^{-6} (0.282)	2.77×10^{-6} (0.160)	2.52×10^{-6} (0.112)
Titanium	50	6.82×10^{-6} (0.277)	6.60×10^{-6} (0.160)	—
	100	7.58×10^{-6} (0.276)	7.02×10^{-6} (0.158)	—
		6.59×10^{-6} (0.279)	6.99×10^{-6} (0.175)	
Platinum	100	17.1×10^{-6} (0.149)	15.0×10^{-6} (0.098)	—

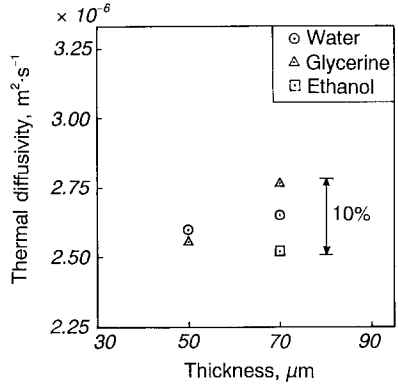

Fig. 8. Experimental results of the thermal diffusivity of stainless steel (SUS304) foils.

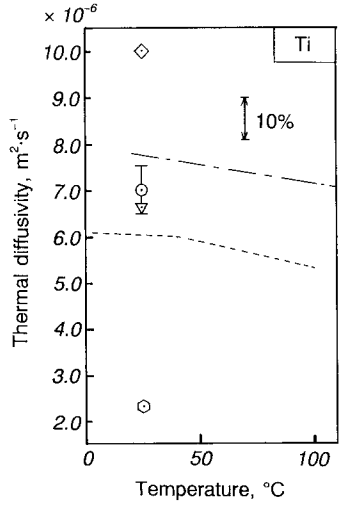

Fig. 9. Comparison between the present experimental thermal diffusivity results and other previous studies for titanium. (◇) Namba et al. [24]; (---) McIntosh et al. [27]; (-·-) Kosaka et al. [25]; (⊙) Steinberg et al. [23]; (▽) Bottani et al. [26]; (⊙) present work.

the applicability of the photoacoustic method to thin samples on backing using the RG theory without any approximations.

Table II summarizes the present results on thermal diffusivity and b. Figure 8 shows that in the case of stainless steel, as an example, the measured thermal diffusivity data agree within $\pm 5\%$ regardless of the sample thickness and backing materials, which implies that the present apparatus was operating in accordance with the theory. In the same way, b values are also reproducible within $\pm 5\%$. Figure 9 compares the present absolute thermal diffusivity values for titanium with other data obtained by different methods. As can be seen in Fig. 9, even for a metal such as titanium, the difference between the data of Steinberg et al. [23] and the data of Namba et al. [24], both obtained by the laser flash method, reaches 500%. This is due mainly to the difference of sample characteristics: heat treatment and purity. For example, the purity of Kosaka and co-workers' [25] sample is 99.88%, with no description of heat treatment, and that Bottani and co-workers' is [26] 99.95% and annealed. The present results, which have a reproducibility of $\pm 7\%$, agree with the data of Bottani et al. obtained by the thermoelastic method and are close to the values of Kosaka et al. obtained by the constant-rate heating method and the data of McIntosh et al. [27] obtained by the periodic heat-flow method. At this time, the accuracy of the present measurements is estimated to be within $\pm 7\%$.

7. CONCLUSIONS

The present study leads to the conclusion that the photoacoustic method has the potential of being applied to measurements of the thermal diffusivity of thin films on substrate under various conditions. To establish the photoacoustic method as a reliable thermophysical properties measurement technique, further studies on the error analysis and assessment of accuracy are currently under way. The final goal of our study on the photoacoustic method is to apply the method to thin films (of the order of micrometers) produced by sputtering or CVD on substrate.

ACKNOWLEDGMENTS

The work described in this paper has been supported in part by the Kurata Foundation and the Yazaki Memorial Foundation for Science and Technology. The authors would like to thank S. Arai for his help during the initial phase of conception and design.

REFERENCES

1. M. Sakamoto, *Denshi Zairyo* **29**:34 (1990) (in Japanese).
2. S. Murata and K. Nishimura, *O plus E* No. 125:135 (1990) (in Japanese).
3. D. L. Decker, L. G. Koshigoe, and E. J. Ashley, *NBS Special Publication 727, Laser Induced Damage in Optical Materials*, (1984), p. 291.
4. A. H. Guenther and J. K. McIver, *Thin Solid Films* **163**:203 (1988).
5. A. H. Guenther and J. K. McIver, *Laser Particle Beams* **7**:433 (1989).
6. J. C. Lambropoulos, M. R. Jolly, C. A. Amsden, S. E. Gilman, M. J. Sinicropi, D. Dialomihalis, and S. D. Jacobs, *J. Appl. Phys.* **66**:4230 (1989).
7. A. Redondo and J. G. Beery, *J. Appl. Phys.* **60**:3882 (1986).
8. H. A. Macleod, *J. Vac. Sci. Technol.* **A4**:418 (1986).
9. P. Nath and K. L. Chopra, *Thin Solid Films* **36**:199 (1976).
10. I. Hatta, Y. Sasuga, R. Kato, and A. Maesono, *Rev. Sci. Instrum.* **56**:1643 (1985).
11. H. Ohta, H. Shibata, and Y. Waseda, *Rev. Sci. Instrum.* **60**:317 (1989).
12. A. Ono, T. Baba, T. Matsumoto, H. Funamoto, A. Nishikawa, and K. Takahashi, *Proc. 2nd Asian Thermophys. Prop. Conf.* (1989), p. 473.
13. T. R. Swimm, *Appl. Phys. Lett.* **42**:955 (1983).
14. A. Lachaine, *J. Appl. Phys.* **57**:5075 (1985).
15. A. Rosencwaig, *Photoacoustics and Photoacoustic Spectroscopy* (Wiley, New York, 1980).
16. A. Mandelis, ed., *Photoacoustic and Thermal Wave Phenomena in Semiconductors* (North-Holland, New York, 1987).
17. P. Hess, ed., *Photoacoustic, Photothermal and Photochemical Processes in Gases* (Springer-Verlag, Berlin, 1989).
18. A. Rosencwaig and A. Gersho, *J. Appl. Phys.* **47**:64 (1976).
19. H. S. Carslaw and J. C. Jaeger, *Conduction of Heat in Solids*, 2nd ed. (Oxford, Great Britain 1959), p. 109.
20. C. A. Bennett, Jr., and R. R. Patty, *Appl. Opt.* **21**:49 (1982).
21. S. Krueger, R. Kordecki, J. Pelzl, and B. K. Bein, *J. Appl. Phys.* **62**:55 (1987).
22. G. Benedetto and R. Spagnolo, *Appl. Phys. A* **46**:169 (1988).
23. S. Steinberg, R. E. Larsen, and A. R. Kydd, US Army Natick Lab. Rep. 2409 (1963). [Taken from Y. S. Touloukian, R. W. Powell, C. Y. Ho, and M. C. Nicolaouo, *Thermophysical Properties of Matter, Vol. 10* (Plenum, New York, 1970), p. 196.]
24. S. Namba, P. H. Kim, and T. Arai, *Jap. J. Appl. Phys.* **36**:661 (1967).
25. M. Kosaka, T. Asahina, and S. Ikuta, *Rep. Gov. Ind. Res. Inst. Nagoya* **27**:107 (1978).
26. C. E. Bottani, G. Caglioti, A. Novelli, and P. M. Ossi, *Appl. Phys.* **18**:63 (1979).
27. G. E. McIntosh, D. C. Hamilton, and W. L. Sibbitt, *Trans ASME* **76**:407 (1954).